ACCURACY OF UNIVARIATE ANALYSIS OF MAJOR, MINOR, AND TRACE ELEMENTS IN DOPED SAMPLES USING SCIAPS Z-300 PORTABLE LIBS. Lindsey M. Rollosson[1,2], Danielle D. Michaud[1,2], Cai R. Ytsma[1], and M. Darby Dyar[1], [1]Dept. of Astronomy, Mount Holyoke College, 50 College St., South Hadley, MA 01075, lrollosson@g.hmc.edu, [2]Harvey Mudd College, 301 Platt Blvd., Claremont, CA 91711.

Introduction: Laser-induced breakdown spectroscopy (LIBS) is an increasingly popular spectroscopic method renowned for its lack of sample preparation, *in situ* analysis, and expansive range of detectable elements. For field use on Earth and extraterrestrial surfaces, these characteristics have been incorporated into portable LIBS instruments (pLIBS) that can generate geochemical predictions seconds after analysis. These instruments could be used by astronauts on sorties, but only if their accuracy can be well demonstrated.

The Mount Holyoke College (MHC) Mineral Spectroscopy Laboratory has previously focused on the geochemical quantification of elements relevant to the ChemCam instrument on Mars Science Laboratory [1-4], but the standard calibration suite [5] and insights derived from that work are also applicable to pLIBS. In this work, we investigate the capability of pLIBS to produce quantitative geochemical analyses using univariate analysis techniques and data collected on a SciAps Z-300 pLIBS.

Sample Selection: Samples used in this study are a subset of rock powders doped with elements suitable for LIBS analysis [5]. Standards chosen for univariate analyses were limited to those with dopant concentrations that are found naturally within common terrestrial rocks and minerals (**Table 1**).

Spectral Acquisition: Spectra were acquired from the same pressed powder pellets (in 1.6 cm aluminum cups) used to calibrate the ChemLIBS instrument at MHC; grain size was <<1 mm, many times smaller than the beam diameter used for ablation. The pLIBS firing window was held flush to each pellet and the GeoChem instrument setting collected spectra on 4×3 plasma arrays at three random locations on each sample surface. The three output spectra (each one an automated average of the 12 spectra array) were exported and averaged to generate one spectrum per sample. These spectra were then normalized by dividing the intensity of each channel by the sum of intensities over the entire spectrum.

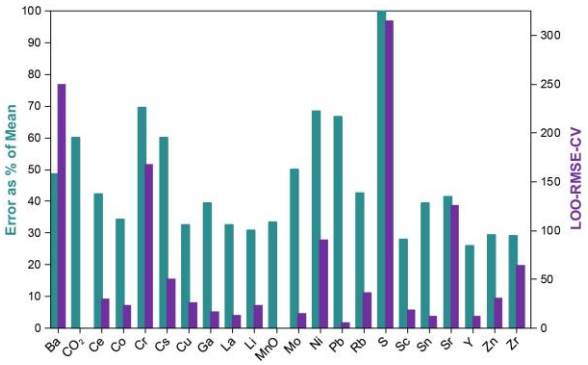

Figure 1. Comparison of LOO-RMSE-CV errors from Table 2 and those errors recast as percentages of the mean concentration of each element.

Peak Selection: For each element, the r^2 correlation between spectra intensity and dopant concentration was used to evaluate the predictive value at each wavelength (23,431 channels over 180–961 nm). Wavelengths with the highest r^2 values were visually inspected to confirm the presence of peaks. These were then cross-checked in NIST's LIBS spectral database [6] to identify the corresponding elemental transition. Predictive accuracy of the two most intense emission peaks reported by NIST (as visible in the spectra) was also evaluated, even when were not located at the wavelength of a high r^2 value. B, Nb, and Se had no well-correlated peaks.

Analysis: OriginPro 9.55 software was used to fit a Voigt peak to each emission feature and calculate the peak area. Peak areas were related to dopant concentrations by linear regression. Leave-one-out cross-validation (LOO-CV), in which a single sample is removed from the regression and its concentration is predicted using the remaining spectra, was used to quantify prediction accuracy. The difference between the model-predicted concentration and the true value of each sample was calculated. This process was performed iteratively for the entire calibration set. The errors incurred by each iteration were used to calculate the root-mean-squared error (RMSE) for each regression line. This analysis was performed on each correlated peak (**Table 2**). The four right-hand columns show the accuracy expressed as LOO-RMSE-CV and as r^2 of the correlation between known and. predicted concentration. The errors are shown as a percentage of the mean concentration in **Figure 1**.

Discussion: Overall, these results demonstrate the same trends seen in earlier work with more sensitive LIBS instruments [3,4]. The geochemical diversity of this suite poses great challenges for univariate peak analysis because of chemical matrix effects. When a sample matrix is unknown, univariate calibration accuracy is limited by how well the calibration matrix is able to match the sample matrix. Mismatch of matrix between standards and unknowns causes large analytical uncertainties, as seen in Table 2. Multivariate analysis [7] shows potential for overcoming this problem.

However, this calibration demonstrates the capability of portable LIBS instruments to produce qualitative

geochemical analyses in the field. More sophisticated calibration models that can produce quantitative analyses are within reach, even with portable instruments.

Acknowledgments: Supported by NSF IIS-1564083, the RIS^{4}E node of the NASA SSERVI NNA14AB04A, and NASA MFRP NNX15AC82G.

References: [1] Tucker J. T. et al. (2010) *Chem. Geol.*, 277, 137-148. [2] Dyar M. D. et al. (2012) *Spectrochim. Acta B*, 70, 51-67. [3] Dyar M. D. et al. (2016) *Spectrochim. Acta B*, 123, 93-104. [4] Lepore K. et al. (2017) *Appl. Spectrosc.*, 7, 1-27. [5] Dyar M. D. et al. (2019) this conference. [6] Kramida, A. et al. *NIST Atomic Spectra Database* (5.5.6) https://physics.nist.gov/asd.

Table 2. Results

Element	N	λ (nm)	Emission Transition	Source	Mean C	LOO-RMSE-CV individual	LOO-RMSE-CV sum	r^2 individual	r^2 sum
Ba	32	455.40	Ba II 6s – 6p	NIST	516	250	252	0.10	0.10
		493.41	Ba II 6s – 6p	NIST		260		0.10	
CO_2	21	193.09	C I $2s^22p^2 – 2s^22p3s$	NIST	0.10	1.02	0.12	-61.00	0.02
		402.03	C I $2s^22p3s – 2s^22p5p$	r^2		0.06		0.46	
Ce	16	769.79	*Y I $4d^25p – 4d^26s$	r^2	71	30		0.25	
Co	10	231.16	Co II $3d^74p – 3d^74d$	NIST	70	28	25	-0.10	-0.03
		238.64	Co II $3d^74s – 3d^74p$	NIST		24		-0.02	
		284.33	*Cr II $3d^44s – 3d^44p$	r^2		32		-0.12	
		293.64	*Mn II $3d^54p – 3d^55d$	r^2		30		-0.17	
Cr	41	359.35	Cr I $3d^54s – 3d^44s4p$	r^2, NIST	242	174	176	0.00	0.00
		360.56	Cr I $3d^54s – 3d^54p$	r^2, NIST		168		0.02	
Cs	20	779.90	Rb I $4p^65s – 4p^65p$	r^2	85	51	52	0.30	0.26
		852.11	Cs I $5p^66s – 5p^66p$	NIST		65		0.02	
		894.35	Cs I $5p^66s – 5p^66p$	NIST		56		0.35	
Cu	15	213.60	Cu II $3d^94s – 3d^94p$	NIST	83	60	40	-0.52	0.09
		324.75	Cu I $3d^{10}4s – 3d^{10}4p$	NIST		672		-300	
		398.97	unknown	r^2		27		0.30	
Ga	10	294.36	Ga I $3d^{10}4s^24p – 3d^{10}4s^24d$	NIST	43	17	21	0.22	0.07
		553.54	*Ba I $6s^2 – 6s6p$	r^2		20		-0.02	
La	13	339.20	*Zr II	r^2	43	15	32	0.51	-0.21
		394.90	La II 5d6s – 5d6p	NIST		21		0.11	
		779.94	Zn I	r^2		14		0.64	
Li	9	610.37	Li I $1s^22p – 1s^23d$	NIST	78	29	24	0.35	0.57
		670.79	Li I $1s^22s – 1s^22p$	r^2, NIST		24		0.53	
MnO	18	257.61	Mn II $3d^54s – 3d^54p$	NIST	0.09	0.06	0.04	-0.01	0.53
		294.92	Mn II $3d^54s – 3d^54p$	NIST		0.06		0.11	
		794.72	O I	r^2		0.03		0.76	
Mo	10	379.82	Mo I $4d^55s – 4d^55p$	NIST	30	20	15	-0.02	0.29
		553.54	*Ba I $6s^2 – 6s6p$	r^2		17		0.07	
Ni	27	221.65	Ni II $3p^63d^84s – 3p^63d^84p$	NIST	133	91	92	0.04	0.03
		239.45	Ni II $3p^63d^84s – 3p^63d^84p$	NIST		93		0.02	
Pb	23	280.26	Pb I $6s^26p^2 – 6s^26p6d$	NIST	9	6		0.02	
Rb	20	779.85	Rb I $4p^65s – 4p^65p$	r^2, NIST	87	37	57	0.49	0.01
		794.76	Rb I $4p^65s – 4p^65p$	NIST		57		0.00	
S	54	922.29	*Mn II $3d^55f – 3d^58g$	NIST	267	315		0.00	
Sc	12	357.26	Sc II $3p^63d4s – 3p^63d4p$	NIST	68	22	20	0.12	0.46
		361.38	Sc II $3p^63d4s – 3p^63d4p$	NIST		27		0.02	
		363.07	Sc II $3p^63d4s – 3p^63d4p$	r^2		30		-0.01	
		437.52	Sc I 3d4s4p – 3d4s4d	r^2		19		0.27	
Sn	11	189.99	Sn II $5s^25p – 5s^26s$	NIST	33	22	25	-0.02	-0.02
		284.00	Sn I $5s^25p^2 – 5s^25p6s$	NIST		33		-0.52	
		894.17	unknown	r^2		13		0.46	
Sr	31	407.77	Sr II $4p^65s – 4p^65p$	NIST	304	501	126	-5.94	0.08
		421.55	Sr II $4p^65s – 4p^65p$	NIST		130		0.10	
Y	12	324.23	Y II 4d5s – 4d5p	NIST	50	23	18	0.04	0.19
		339.20	unknown	r^2		71		0.64	
		779.90	*Rb I $4p^65s – 4p^65p$	r^2		13		0.58	
Zn	20	300.03	*Co I $3p^63d^74s^2 – 3p^63d^84p$	r^2	105	43	40	0.17	0.45
		532.82	unknown	r^2		31		0.59	
Zr	19	262.06	Zr III 4d5s – 4d5p	NIST	223	100	65	0.06	0.66
		264.40	Zr III 4d5s – 4d5p	NIST		102		0.01	
		779.90**	*Rb I $4p^65s – 4p^65p$	r^2		66		0.64	

Concentrations reported as ppm except where given as oxide. N = number of samples. Mean C = mean concentration of that element in all samples used in its calibration. * = elements in same doping suite. **Gaussian fit.